FEMS Microbiology Ecology Advance Access published October 22, 2015

Confocal Raman microspectroscopy reveals a convergence of the chemical composition in methanogenic archaea from a Siberian permafrost-affected soil

Paloma Serrano[1, 2], Antje Hermelink[3], Peter Lasch[3], Jean-Pierre de Vera[4], Nicole König[3], Oliver Burckhardt[1], Dirk Wagner[1#]

[1] GFZ German Research Centre for Geosciences, Helmholtz Centre Potsdam, Section Geomicrobiology, Telegrafenberg, 14473 Potsdam, Germany.

[2] Alfred Wegener Institute Helmholz Centre for Polar and Marine Research. Telegrafenberg A45 14473 Potsdam, Germany.

[3] Robert Koch Institute. Centre for Biological Threats and Special Pathogens; Nordufer 20 13353 Berlin, Germany.

[4] German Aerospace Center (DLR) Berlin, Institute of Planetary Research. Rutherfordstraße 2 12489 Berlin, Germany.

corresponding author: Dirk Wagner, GFZ German Research Centre for Geosciences, Helmholtz Centre Potsdam, Section Geomicrobiology, Telegrafenberg, 14473 Potsdam, Germany

Tel: +49 331 288 28800

Fax: +49 331 288 28802

Email: Dirk.Wagner@gfz-potsdam.de

Keywords: methanogenic archaea, Siberian permafrost, confocal Raman microspectroscopy, chemical composition, environmental adaptations, *mcrA*.

Running title: Chemical convergence in methanogens from Siberian permafrost

Abstract

Methanogenic archaea are widespread anaerobic microorganisms responsible for the production of biogenic methane. Several new species of psychrotolerant methanogenic archaea were recently isolated from a permafrost-affected soil in the Lena delta (Siberia, Russia), showing an exceptional resistance against desiccation, osmotic stress, low temperatures, starvation, UV and ionizing radiation when compared to methanogens from non-permafrost environments. To gain a deeper insight into the differences observed in their resistance, we described the chemical composition of methanogenic strains from permafrost and non-permafrost environments using confocal Raman microspectroscopy (CRM). CRM is a powerful tool for microbial identification and provides fingerprint-like information about the chemical composition of the cells. Our results show that the chemical composition of methanogens from permafrost-affected soils presents a high homology and is remarkably different from strains inhabiting non-permafrost environments. In addition, we performed a phylogenetic reconstruction of the studied strains based on the functional gene *mcrA* to prove the different evolutionary relationship of the permafrost strains. We conclude that the permafrost methanogenic strains show a convergent chemical composition regardless of their genotype. This fact is likely to be the consequence of a complex adaptive process to the Siberian permafrost environment and might be the reason underlying their resistant nature.

Introduction

Methanogenic archaea are strictly anaerobic microorganisms that belong to the phylum *Euryarchaeota* and produce methane as an obligate catabolic end-product (Ferry, 1993). About 85 % of the annual global methane formation is mediated by methanogenic archaea

(Thauer *et al.*, 2008). Once released, methane can either be oxidized in biotic and abiotic processes or accumulate in the Earth's atmosphere as a greenhouse gas, where it will slowly oxidize by means of photochemical reactions. The atmospheric methane concentration has increased more than twofold in the last 200 years (Hedderich & Whitman, 2006), contributing to the increase in the Earth's temperature over the last decades.

Terrestrial permafrost predominantly occurs in the northern hemisphere and covers approximately 24 % of Earth's land surface. It represents a significant natural source of methane, largely of biological origin (Fung *et al.*, 1991, Wagner *et al.*, 2003). Arctic tundra soils in Siberia are permanently frozen throughout the year with the exception of the thin active layer, subjected to seasonal freeze-thaw cycles with *in situ* temperatures ranging from -45°C to 25°C (Wagner *et al.*, 2005). Several novel strains of psychrotolerant methanogenic archaea were recently isolated from the active layer of a permafrost-affected soil in the Lena Delta (Siberia, Russia). Unlike psychrophiles, psychrotolerant methanogens show a broad adaptive potential to the fluctuating environmental conditions, including a wide temperature range and the subsequent geochemical gradients (Simankova *et al.*, 2003) as it can be observed in the active layer of the permafrost environment. Previous experiments in our labs have demonstrated the remarkable resistance of Siberian permafrost methanogenic strains against desiccation, osmotic stress, low temperatures and starvation when compared to methanogenic archaea from non-permafrost environments (Morozova & Wagner, 2007, Wagner *et al.*, 2013). They also exhibit a high level of resistance to monochromatic and polychromatic UV and ionizing radiation (D. Wagner, unpublished data), comparable to that of *Deinococcus radiodurans* (Brooks & Murray, 1981). In addition, methanogens from Siberian permafrost environments are able to survive simulated Martian thermo-physical conditions (Morozova *et al.*, 2007) and simulated Martian subsurface analog conditions (Schirmack *et al.*, 2013), in contrast to other psychrophilic methanogens from non-

permafrost habitats such as *Methanogenium frigidum* (Franzmann *et al.*, 1997) from Ace Lake, Antarctica, which cannot resist these conditions (Morozova *et al.*, 2007). Among the Siberian permafrost isolates, the genera *Methanosarcina* and *Methanobacterium* are broadly represented. *Methanosarcina* can metabolize a broad spectrum of substrates, including hydrogen, methanol and acetate (Liu & Whitman, 2008). *Methanobacterium* species present a hydrogenotrophic metabolism, growing on H_2+CO_2 or formate (Ferry, 1993).

The reasons why psychrotolerant methanogens from Siberian permafrost environments are more resistant to a broad range of extreme parameters than their relatives from psychrophilic and mesophilic non-permafrost habitats remains unknown. We hypothesize that this difference might depend on specific adaptations reflected in their biomolecules. In order to investigate the chemical composition of methanogens from Siberian permafrost and non-permafrost habitats, we used a Raman spectroscopy setup. Raman spectroscopy is a vibrational spectroscopic technique that provides fingerprint-like information about the overall chemical composition of the cell and requires a minimal sample preparation, allowing a rapid nondestructive investigation (Rösch *et al.*, 2005, Harz *et al.*, 2009). The strains in this study were previously investigated by Fourier-transformed Raman spectroscopy in an attempt to perform a bulk analysis of their chemical composition. However, due to the nature of the cells and the presence of metabolic byproducts (Serrano *et al.*, 2013), confocal Raman microspectroscopy (CRM) proved to be the optimal method. CRM combines a dispersive Raman setup with a high-numerical aperture confocal microscope, enabling the study of the chemical structure and composition of individual cells under diffraction-limited conditions (Krause *et al.*, 2008, Hermelink *et al.*, 2009). This technique has allowed the characterization of the chemotaxonomic features in multiple microorganisms to the species and even strain level (Maquelin *et al.*, 2002).

Additionally, a phylogenetic reconstruction based on the gene *mcrA* was performed to investigate the phylogenetic relationships among the strains in this study. Microbial phylogenetics is often based on the 16S rRNA molecule, although other important molecular markers for classification are known. In methanogenic archaea, the functional gene *mcrA* codes for the α subunit of the methyl coenzyme-M reductase (*MCR*), which catalyzes the last step of the methanogenesis (Ferry, 2010). MCR is thought to be unique to methanogens and, since it retains a common function, sequence comparisons are considered to provide valid phylogenetic data (Reeve, 1992). The gene *mcrA* has also proven to be an alternative to 16S rRNA in the phylogenetic analysis of methanogen populations (Luton *et al.*, 2002).

In this study, we describe the overall chemical composition of three strains of methanogens from Siberian permafrost and two strains of methanogens from non-permafrost habitats by means of CRM in an attempt to gain insights into their different resistance to extreme and fluctuating environmental parameters. In addition, we give a phylogenetic overview of the studied strains and their evolutionary relationship based on the functional gene *mcrA*. Finally, we discuss the differences in the chemical nature in relation to the reconstructed phylogeny.

Materials and Methods

Archaeal cultures

The three psychrotolerant methanogenic strains from Siberian permafrost environments used for this study were *Methanosarcina soligelidi* SMA-21 (Wagner *et al.*, 2013), SMA-17 and SMA-27. They were isolated from the active layer of permafrost-affected soils in the Lena Delta, Siberia (Russia). In nature, they thrive in temperatures ranging from -45ºC to +25ºC and even if they can grow at temperatures down to 0°C, the optimal growth temperature of

the isolates is 28ºC. *Ms. soligelidi* SMA-21 (DSM 26065^{T}) and SMA-17 appear as irregular cocci, ~1µm in diameter and cell aggregation is often observed. They show 99.9 % homology on the 16S rRNA sequence with *Methanosarcina mazei* (Mah, 1980). SMA-27 cells are elongated rods, ~3-4 µm long. Their closest relative according to the 16S rRNA molecule is *Methanobacterium congolense (Cuzin et al., 2001) (*96.4 % homology. Wagner, unpublished). Additionally, two mesophilic strains from non-permafrost habitats were used as reference strains. *Ms. barkeri* DSM 8687 originates from a peat bog in northern Germany (Maestrojuan *et al.*, 1992) and *Ms. mazei* DSM 2053 was isolated from a mesophilic sewage sludge plant in California, USA. Both strains were obtained from the German Culture Collection of Microorganisms and Cells (DSMZ, Braunschweig, Germany), appear as irregular cocci, ~1µm in diameter, grow in colonies and are found in diverse environments. Both show an empirical optimal growth at the temperature of 28ºC.

Growth conditions of methanogenic strains

For an accurate comparison of the spectra, the Raman measurements were performed in living cells from pure cultures grown at optimal conditions at 28^{0}C and at their stationary phase of growth (approximately 3 weeks after innoculating the cultures). The permafrost strains were not grown at simulated permafrost conditions for the following reasons: 1) permafrost conditions are extremely difficult to simulate, considering the yearly long term freezing and thawing cycles, that consequently cause changes in the salinity and the geochemical gradients, very difficult to accurately simulate in culture conditions. 2) The freezing and thawing cycles that would partly recreate permafrost conditions would cause environmental stress on the cells due to the changing parameters. Therefore, the permafrost populations would contain less viable healthy cells and the quality of the cultures between fresh non-permafrost cultures and aged permafrost cultures exposed to environmental stress would not allow a fair comparison of the chemical composition.

Pure cultures were grown in sealed bottles that contained 50 mL of MW medium [(L^{-1}): NH_4Cl 0.25 G, $MgCl_2$ x $6H_20$, 0.4 G, $CaCl_2$ x $2H_2O$ 0.1 G, KCl, 0.5 G, KH_2PO_4, 0.2 G, Na HCO_3, 2.7 G, Cysteine, 0.3 G, Na_2S, 0.2 G; trace element solution (Balch *et al.*, 1979), 10mL; vitamin solution (Bryant *et al.*, 1971), 10mL] in *Methanosarcina* strains and CS medium [(L^{-1}): NH_4Cl, 0.3 G, $MgCl_2$ x $6H_2O$, 0.4 G, $CaCl_2$ x $2H_2O$, 0.16 G, NaCl, 1.0 G, KCl, 0.5 G, K_2HPO_4 0.25 G, Na HCO_3, 2.7 G, Na-Acetate, 0.25 G, $Na_2S_2O_4$, 0.1 G, Na_2S, 0.25 G; trace element solution (Imhoff-Stuckle & Pfennig, 1983), 1mL; vitamin solution (Bryant *et al.*, 1971), 1mL] in the case of SMA-27 (since the growth of SMA-27 in MW medium was suboptimal). Both media contain 2 mL resazurin (7-Hydroxy-3H-phenoxazin-3-on-10-oxide). The bottles were flushed and pressurized to one atmosphere with H_2/CO_2 (80:20 v/v). For sample preparation, 200 mL from four sets of pure cultures in the stationary phase of growth were centrifuged at 7900 g for 40 min and 4°C and washed twice in 200 mL of distilled water at 4600 g for 30 min and 4°C. 7 µL of the cell suspensions were air-dried onto a CaF_2 slide, previously diluted 1:10 and 1:100 for a better observation of the single cells.

Raman microspectroscopy

Raman spectra were captured using a WITec (Ulm, Germany) Model alpha 300R confocal Raman microspectroscope (CRM), calibrated according to the manufacturer's instructions with an Ar/Hg spectral lamp. The CRM contained an ultra-high throughput spectrometer (UHTS300) and used a back-illuminated EMCCD camera (Andor Technology PLC, Belfast, Northern Ireland) as detector. All the measurements presented in this article were performed with an apochromatic Nikon E Plan (100x/0.95) objective (Tokyo, Japan) and a working distance of 0.230 mm at an excitation wavelength of 532 nm (frequency doubled Nd-YAG laser; 35mW laser power). A minimum of 20 individual cells were measured, each of them

with 5s of accumulation time under full pixel binning and without gaining at the camera. Further technical details about the Raman equipment and measurements were reported in detail in Serrano *et al.* (2014).

For hierarchical clustering of the CRM spectra, a cosmic ray removal procedure was first performed on the spectra, followed by the individual export of each spectrum via an ASCII interface into OPUS 5.5 (Bruker Optik GmbH, Rheinstetten, Germany). As part of the pre-processing, we carried out a quality test in order to assess the signal-to-noise ratio and a pre-selection of the cell-based spectra that contains the principal components of the spectrum. The first derivative with Savitzky-Golay smoothing/ derivative filter was applied using 9 smoothing points and normalized vectors. Spectral distances between pairs of individual spectra were obtained based on the data from the 796-1854 and 2746-3205 cm^{-1} spectral regions as D-values (Naumann, 2000) derived from normalized Pearson's product momentum correlation coefficient. The normalization allows a variation between D-value=0 (r=1: high correlated data/identity), D-value=1000 (r=0: uncorrelated data) and D-value=2000 (r=-1:anti-correlated spectra) and prevents negative values (Helm *et al.*, 1991). Average linkage was used as the clustering method. For the cluster analysis in Figure 4A, the same method was applied to the average spectra obtained from averaging the individual spectra of each strain shown in Fig. 2, including the outlying spectra.

The individual Raman intensities of all strains within the regions of 850 - 1850 and 2750 - 3200 cm^{-1} were treated as statistical variables and subjected to a rigid rotation via a Principal Component Analysis (PCA) using the commercial software package MATLAB R2014a (The Mathworks Inc, Natick, MA). This allows for the reduction of the original variables into fewer, independent variables and to visualize and compare spectra between permafrost and non-permafrost methanogenic strains.

Phylogenetic analysis

For phylogenetic analysis based on the *mcrA* sequence, the DNA was extracted from pure cultures of the five mentioned strains following the user manual of the UltraClean® DNA purification kit. The mcrA gene (Bokranz *et al.*, 1988) was amplified with the primers ME1 (forward: gCMATgCARATHggWATgTC) and ME2 (reverse: TCATKgCTAgTTDggRTAgT). The PCR consisted in 32 cycles of 1min at 94ºC (denaturation) followed by 1 min at 55ºC (annealing) and 1 min at 72ºC (elongation). A previous denaturation stage (10min, 95ºC) and a final elongation (10min, 72ºC) were performed, resulting in a 710 base pairs gene product. Sequencing was performed by GATC Biotech (Constance, Germany). The consensus sequence was obtained using the software CodonCode Aligner (Codoncode Cooperation, MA, USA). The nucleotide sequences from the Siberian permafrost strains were uploaded in GeneBank under the numbers KJ432634 (*mcrA Ms. soligelidi* SMA-21), KJ432635 (*mcrA* SMA-17) and KJ432633 (*mcrA* SMA-27).

A multiple alignment of the five *mcrA* sequences was performed with ClustalW (Thompson *et al.*, 1994) through Geneious pro 5.6.6 (Biomatters Ltd.) and a maximum likelihood tree (1000 bootstraps) was built using the GTR substitution model including the methanogenic archaea *Methanopyrus kandleri* (Kurr *et al.*, 1991) order *Methanopyrales*, (Genbank U57340) as an outgroup.

Results

Raman spectra of permafrost and non-permafrost methanogens

The Raman spectra of the analyzed strains *Ms. soligelidi* SMA-21, SMA-17 and SMA-27 from Siberian permafrost and *Ms. barkeri* and *Ms. mazei* from non-permafrost habitats are illustrated in Figure 1 and described Table 1. The highest Raman intensity in all spectra was

the CH_2 stretching vibration around 2936 cm^{-1}. The spectra from permafrost strains exhibited a shoulder at 2885 cm^{-1}, which corresponds to the symmetric CH_3 stretching (Socrates, 2004), indicating significant differences in the aliphatic chain composition between permafrost and non-permafrost methanogenic strains. Raman modes of proteins were found at 1669 cm^{-1} (amide I) and at 1243-1275 cm^{-1} (region of amide III). Their intensities are correlated and show slightly lower values for *Ms. soligelidi* SMA-21 and SMA-17. The peak at 1610 cm^{-1} corresponds to the bond C=C found in aromatic amino acids phenylalanine and tyrosine and reached higher intensities in non-permafrost strains, whereas the peak at 1589 cm^{-1} is associated to the ring breathing modes of ribonucleotides guanine and adenine as well as the amino acid tryptophan and was absent in permafrost strains. The intensity of the 1460 cm^{-1} band, attributed to CH_2 deformation, was similar in all strains investigated. The peaks at 1344 cm^{-1} and 1338 cm^{-1} were both assigned to the deformation of the group CH in carbohydrates and proteins (Ivleva *et al.*, 2009). The peak at 1344 cm^{-1} reached the highest intensity for *Ms. mazei*, the lowest for *Ms. soligelidi* SMA-21 and SMA-17 and intermediate values for SMA-27 and *Ms. barkeri*, whereas the one at 1338 cm^{-1} was unique to the permafrost strains SMA-21 and SMA-17. All the mentioned bands varied slightly in bandwidth, position and intensity for each strain. The peaks in the spectral region located between 1200 and 800 cm^{-1} showed relative higher intensities in permafrost strains than in non-permafrost strains, including the bands located at 1167 cm^{-1} (C-C and C-O ring breathing), 1128 cm^{-1} (characteristic of the C-O-C in the glycosidic link) and 1054 cm^{-1} (C-O and C-C from carbohydrates, and C-C and C-N in proteins, Neugebauer *et al.*, 2007). The band at 1008 cm^{-1} was attributed to the symmetric benzene/ pyrrole in-phase and out-of-phase breathing modes of phenylalanine (Ivleva *et al.*, 2009). The band at 860 cm^{-1} corresponded to the C-C stretching modes and the C-O-C glycosidic link in polysaccharides (Pereira *et al.*, 2004), and the peak at 835 cm^{-1} was exclusive to the permafrost strains and

was attributed to the ring breathing of the amino acid tyrosine and the group O-P-O present in nucleic acids (Ivleva *et al.*, 2009).

The cluster analysis based on the Raman spectra showed the similarities and differences in the overall chemical composition of permafrost and non-permafrost strains in stationary phase, revealing two chemically different clusters illustrated in Figure 2 (individual spectra) and 4A (average spectra). CRM spectra corresponding to individual cells of the same microbial strain clustered together, with the exception of two spectra from SMA-27 and three spectra from *Ms. soligelidi* SMA-21 (Fig. 2). The outlying spectra of SMA-27 were equally distant to the spectra of the SMA-27 cluster and the *Ms. soligelidi* SMA-21/ SMA-17 cluster, separated by the distance of 104.6 and 123.1 D-value units, respectively. Three outlying spectra of *Ms. soligelidi* SMA-21 were separated by 70.8 D-value units from the *Ms. soligelidi* SMA-21/ SMA-17 cluster. Spectra from *Ms. mazei*, *Ms. barkeri* and SMA-17 cells were less heterogeneous and grouped into unique clusters at the strain level.

The cluster analysis in Figure 4A shows an overview of the phenotypic resemblance in the chemical composition based on the average spectra of each strain, obtained from averaging the individual spectra, including the outliers (and therefore disregarding the intraspecific variances in the heterogeneity). Strains *Ms. soligelidi* SMA-21 and SMA-17 were most similar, separated by 15.6 D-values. The cluster *Ms. soligelidi* SMA-21/ SMA-17 was closely related to the strain SMA-27, also from Siberian permafrost, distanced by 37.8 D-values. Apart from the permafrost group, the spectra from *Ms. mazei* and *Ms. barkeri* (non-permafrost strains) grouped together, separated by 24.4 D-value units. The total distance between the permafrost and the non-permafrost cluster was 84.4 D-values.

The PCA in Figure 3A shows the score plot of the first 3 principal components (PCs) that cumulatively captured 88.04 % of the total variance in the spectral regions of interest. It demonstrated that each strain occupies a distinct variable space, forming non-overlapping

data clouds. Additionally, PC1 can effectively separate the permafrost and the non-permafrost groups (note that PCA has been carried out on normalized spectra), illustrating shared spectral features within each of the two groups and divergent spectral features between these groups. Figure 3B shows the loadings of the first three PCs. PC1 (62.72% of the variance) is dominated by strong bands at the labeled wavelengths, which correspond to the vibrational modes of proteins, carbohydrates, nucleic acids and lipids (Neugebauer *et al.*, 2007, Ivleva *et al.*, 2009) and illustrate additional differences within the chemical composition between permafrost and non-permafrost strains. The downward peaks correspond to distinct features shared by non-permafrost methanogens, whereas the upward peaks correspond to shared features of permafrost methanogens.

Phylogenetic relationships of methanogenic archaea

A maximum likelihood tree (GTR substitution model, 1000 bootstraps) was built for the studied methanogens according to the *mcrA* nucleotide sequence, using *Methanopyrus kandleri* as the outgroup (Fig. 4B). All the *Methanosarcina* species clustered together, with *Ms. soligelidi* SMA-21 and SMA-17 from the Siberian permafrost showing identical *mcrA* sequences. The cluster *Ms. soligelidi* SMA-21/ SMA-17 was closely related to *Ms. mazei*, sharing a 98.5 % identity in their sequences. *Ms. mazei* and *Ms. barkeri* presented a 91.5 % homology. Finally, SMA-27 was the most evolutionary distant strain, sharing only 61% of the *mcrA* nucleotide sequence with the rest of the studied strains.

Discussion

Previous studies have shown that methanogenic archaea from permafrost habitats are more tolerant to different environmental stress factors compared to those from non-permafrost

areas (Morozova *et al.*, 2007, Morozova & Wagner, 2007, Morozova *et al*., 2015). In this study, we have shown that Siberian permafrost and non-permafrost strains could be classified into two different groups according to their chemical composition on the basis of CRM analysis. The Siberian permafrost strains *(Ms. soligelidi* SMA-21, SMA-27 and SMA-17) show a higher degree of similarity in their chemistry and the spectral clusters of SMA-27 and *Ms. soligelidi* SMA-21 present outlying spectra, suggesting that their populations are more chemically heterogeneous than the other strains (Fig. 2). However, the high phenotypic heterogeneity within a cell population and diversity between different growth phases described for *Ms. soligelidi* SMA-21 (*Serrano et al.*, (2014) were also observed in all the strains investigated in this study. When comparing the cluster analysis of the individual spectra (Fig. 2) with the average spectra (Fig. 4A), two puzzling facts concerning the scale, and therefore the heterogeneity, were observed: (i) The scales were different, despite referring to the same data; (ii) The heterogeneity within the SMA-27 population was larger than the overall distance in the average spectra. The explanation relies on the fact that the average spectra were obtained by averaging the single spectra from each strain, including the outliers, which considerably increased the variance of the corresponding strains (*Ms. soligelidi* SMA-21 and most remarkably SMA-27). The largely different variances within each strain were therefore not proportionally weighed for the cluster analysis of the average spectra and, despite this fact, the permafrost and the non-permafrost strains cluster in different groups according to their chemical composition.

The clusters resulting from the PCA of the individual spectra (Fig. 3A) support the cluster analysis in Figure 2, evidencing that CRM can be used to differentiate between strains, which form non-overlapping data clouds on the plot. Furthermore, the first principal component has separated out permafrost from non-permafrost strains. However, the Raman-spectroscopic differences between permafrost and non-permafrost strains (Fig. 1 and 3B) are

non-conclusive when it comes to pointing to specific biomolecules that differentiate the two groups. Raman spectroscopy exclusively shows the differences in the vibrational modes and thus in the chemical composition, without revealing the biomolecule itself. For example, the band at 2885 cm^{-1} (Fig. 1) corresponds to the symmetric CH_3 stretching, indicating significant differences in the aliphatic chain composition between permafrost and non-permafrost methanogens, but this technique does not allow for the identification of specific phospholipids.

On the other hand, the evolutionary relationships among the strains do not correspond in all cases with the topology found for the chemical composition. The phylogenetic relationship provided by the gene *mcrA* proves that the permafrost strains do not form a monophyletic group (Fig. 4B). The *mcrA* sequences of *Methanosarcina* strains from the Siberian permafrost (SMA-21 and SMA-17) are closely related to each other, whereas SMA-27 presents only 61% of homology with the rest of the strains and aligned with the genus *Methanobacterium*. Sequence alignments of the 16S rRNA molecule corroborate these findings (Wagner, unpublished), evidencing that SMA-27 forms a distantly-related sister group. The non-permafrost strains, *Ms. mazei* and *Ms. barkeri*, share a remarkable degree of homology in both chemical composition and genetic information. The maximum likelihood analysis based on *mcrA* shows a full bootstrap support for the node that separates *Ms. barkeri* (Fig. 4B). Although the other two nodes within that group are not completely resolved, it is evidenced that *Ms. mazei* is the most closely related strain to *Ms. soligelidi* SMA-21 and SMA-17.

This study proves that Siberian permafrost methanogenic strains share a related chemistry, regardless of their evolutionary origin. In other words, methanogens with different genotypes can exhibit an analogous phenotype in terms of chemical composition. This finding points to the evidence of the complexity of the adaptations to the environmental conditions,

suggesting that methanogenic strains from Siberian permafrost may have developed common biochemical adaptations to sub-zero temperatures, freeze-thaw cycles, osmotic stress and high levels of background radiation over geological time scales. A plausible phenomenon explaining the convergent chemical composition in permafrost strains despite their different genotype is the horizontal gene transfer (HGT) (Jain *et al.*, 1999). HGT allows the rapid incorporation of novel functions that provide a selective advantage to the organism and there is proof of HGT in the evolution of some genes coding for enzymes involved in methanogenic pathways (Fournier, 2009). The Alien Hunter programme (Vernikos & Parkhill, 2006) predicted that between 35% and 51% of the genome of methanogenic archaea has undergone HGT, and the highest percentage corresponded to the psychrophilic archaeon *Methanococcoides burtonii* (Allen et al., 2009). However, the gene *mcrA* chosen for this study is not affected by this phenomenon. All *mcr* operons appear to have evolved from a common ancestor and since MCR plays a key role in the methanogenesis, it is highly conserved and provides valid phylogenetic information, independent of the 16S rRNA information (Reeve, 1992). Despite this fact, other operational genes involved in perhaps anabolic pathways may have experienced HGT with the consequent production of molecules/metabolites that might have provided a selective phenotypic advantage to the cells. That selective advantage would enable them to survive in the Siberian permafrost environment and leading to a convergent chemical phenotype of the methanogenic archaea. The specific biomolecules that are different for permafrost and non-permafrost strains and may provide the selective advantage, however, cannot be discriminated by means of CRM.

CRM allows the discrimination between molecules based on their specific vibrational modes. When investigating the composition of a single cell, CRM can be used to describe only the Raman-active biomolecules such as molecules containing aromatic rings

(phenylalanine, tryptophan, pigments etc.), but this technology does not allow the identification of specific biomolecules (e.g. a particular protein or carbohydrate).

Figure 1 and Table 1 illustrate both the quantitative (band intensities) and qualitative (band position) chemical differences found between spectra of permafrost (psychrotolerant) and non-permafrost (mesophilic) methanogens cultured at their optimal conditions and growth temperature (28ºC). Some peaks experience a slight shift in comparison to their standard value in the literature (e.g. the symmetric benzene/ pyrrole in-phase and out-of-phase breathing modes of phenylalanine appear at 1008 cm^{-1} in contrast to Ivleva *et al.*, 2009, with the same peak described at 1003cm^{-1}). Although the calibration of the spectrometer was verified once a week, calibration errors of 3-5 wavenumber units (deviation of approximately one pixel of the 1024 x 128 CCD element) cannot be excluded. However, a systematic calibration error of the CRM measurements is expected to only exert a minor effect on the results of cluster or principal component analysis. Furthermore, the Raman peaks illustrating the differences between the permafrost and non-permafrost groups are not identical in Fig. 1 and Fig. 3B, although they are focused in the same major spectral regions. For instance, the region 1571-1690 cm^{-1} in the average spectra (Fig.1) contains minor fluctuations that correlate with the peaks identified on the PCA (Fig. 3B). This spectral region corresponds to proteins (amide I, 1669cm^{-1}) and aromatic amino acids, and evidences differences between permafrost and non-permafrost strains. The same fact is observed within the region 2846 - 2959 cm^{-1} (Fig. 1), which corresponds to lipids: multiple additional differences in the vibrational modes of permafrost and non-permafrost methanogens are revealed within that region on the PCA (Fig. 3B).

The underlying compositional differences might be correlated with convergent biochemical adaptations to the Siberian permafrost environment and could explain the resistant nature of the permafrost strains when compared to other non-permafrost methanogens. These

adaptations to the Siberian permafrost environment might be related to one or multiple adaptive mechanisms to cold, radiation, desiccation, osmotic stress, and their corresponding seasonal fluctuations. The adaptive mechanisms described for psychrotolerant methanogenic archaea include modifications in cellular components and functional machinery or proteins in order to maintain their structural flexibility and activity under cold temperatures and changing conditions (Dong & Chen, 2012). For instance, the membrane lipids show increasing levels of unsaturation of the fatty acids (Cavicchioli *et al.*, 2000). In Figure 1, the peak at 2936 cm^{-1} (CH_2 stretching region) presents a similar intensity for all strains, pointing to the fact that the lipid content is comparable. Next to it, the peak at 2885 cm^{-1} (symmetric CH_3 stretching) reveals a noticeable contrast between permafrost and non-permafrost strains, denoting qualitative differences in the aliphatic chain composition of the lipids (Socrates, 2004), even when growing at mesophilic temperatures. In addition, previous studies have reported that proteins in psychryotolerant methanogens present a reduced hydrophobic core and a less charged protein surface (Reed *et al.*, 2013), as well as cold-adaptive chaperone proteins, such as Csp, CSD and TRAM domain proteins (Giaquinto *et al.*, 2007). This study shows that the protein levels are slightly more abundant in non-permafrost strains and SMA-27, according to the amide I (1669 cm^{-1}) and amide III bands (1275-1243 cm^{-1}), which correspond to the peptide bond of proteins. On the other hand, the peak at 1610 cm^{-1} is unique to phenylalanine and tyrosine and it is more abundant in non-permafrost strains. However, the peak at 1008 cm^{-1}, assigned to phenylalanine, is slightly higher in the permafrost methanogenic strains. The peaks at 1589 cm^{-1} and 835 cm^{-1} correspond also to aromatic amino acids, but are not unique to them. These findings are in principle compatible with the reduced hydrophobic cores of proteins in psychrotolerant methanogens found by Reed *et al.* (2013), since the proteins from permafrost methanogenic strains present relatively less aromatic (and hydrophobic) amino acids, with the exception of phenylalanine. Unfortunately, only the aromatic amino acids tryptophan, tyrosine and phenylalanine

produce Raman scattering, and therefore this technique does not allow further amino acid identification.

Particularly interesting is the band at 860 cm^{-1}, which is especially prominent in permafrost strains and was previously assigned to the C-O-C 1,4-glycosidic link present in carbohydrates and polysaccharides (Pereira *et al.*, 2004, Ivleva *et al.*, 2009). This distinctive band together with the band at 1338 cm^{-1} confirms the presence of polysaccharide of similar nature in permafrost strains. Many microorganisms, including archaea, have been reported to produce exopolysaccharides (EPSs, sugar-based polymers that are secreted by microorganisms to the surrounding environment) as a strategy to survive adverse conditions (Poli *et al.*, 2011). In fact, they have been shown to play a protective role against desiccation (Ophir & Gutnick, 1994), which might be the case of the permafrost methanogenic strains in the perennially frozen ground or frozen period of the active layer.

In conclusion, this study presents proof of concept that distantly related methanogens (*Methanosarcina* and *Methanobacterium)* occurring in the same habitat have independently developed similarities in the chemical composition (Hoover & Pikuta, 2009). Extreme conditions such as sub-zero temperatures and osmotic stress generally affect macromolecule structures and the thermodynamics of chemical reactions, having the same impact on all microorganisms. Hence, microorganisms that inhabit in the same extreme environment have proven that the features and adaptations that unite them as a group are stronger than the variation imposed by their phylogeny (Cavicchioli, 2006). The microbial communities of permafrost environments have been often referred to as a “community of survivors” (Friedmann, 1994) that have found themselves trapped in this environment and have outcompeted those unable to withstand the given environmental conditions through a process of continuous selection that lasted millions of years (Gilichinsky *et al.*, 1993). The Siberian

permafrost methanogenic strains in this study corroborate the convergence of a certain phenotype in response to the surrounding environment, independent of the genotype.

Acknowledgements

The authors acknowledge Christoph Liedtke (University of Basel) and Susanne Liebner (GFZ German Research Centre for Geosciences) for advice on phylogenetic reconstructions and Mashal Alawi (GFZ German Research Centre for Geosciences) for his comments on the manuscript. The authors declare no conflicts of interest. This work was supported by the Federal Ministry of Economics and Technology (BMWi) by a grant to DW (50WB1152).

References

Allen M, Lauro F, Williams T, *et al.* (2009) The genome sequence of the psychrophilic archaeon, Methanococcoides burtonii: the role of genome evolution in cold adaptation. *ISME Journal* **3**: 1012–1035.

Balch W, Fox G, Magrum L and Wolfe R. (1979) Methanogens: reevaluation of a unique biological group. *Microbiol Rev* **43**: 260-296.

Bokranz M, Baumner G, Allmansberger R, Ankel-Fuchs D and Klein A (1988) Cloning and characterization of the methyl coenzyme M reductase genes from Methanobacterium thermoautotrophicum. *J Bacteriol* **170**: 568-577.

Brooks BW & Murray RGE (1981) Nomenclature for "*Micrococcus radiodurans*" and other radiation-resistant cocci: Deinococcaceae fam. nov. and Deinococcus gen. nov., including five species. *Int J Syst Bacteriol* **31**: 353-360.

Bryant MP, Tzeng SF, Robinson JM & Joyner Jr. AE (1971) Nutrient requirements of methanogenic bacteria. *Adv Chem Ser* **105**: 23-40.

Cavicchioli R (2006) Cold-adapted archaea. *Nature Rev Microbiol* **4**: 331-343.

Cavicchioli R, Thomas T & Curmi PMG (2000) Cold stress response in Archaea. *Extremophiles : life under extreme conditions* **4**: 321-331.

Cuzin N, Ouattara AS, Labat M & Garcia J (2001) *Methanobacterium congolense* sp. nov., from a methanogenic fermentation of cassava peel. *Int J Syst Evol Microbiol* **51**: 489 - 493.

Dong X & Chen Z (2012) Psychrotolerant methanogenic archaea: diversity and cold adaptation mechanisms. *Science China Life Science* **55**: 415-421.

Ferry JG (1993) *Methanogenesis. ecology, physiology, biochemistry and genetics*. Chapman and Hall, New York, London.

Ferry JG (2010) The chemical biology of methanogenesis. *Planet Space Sci* **58**: 1775-1783.

Fournier G (2009) Horizontal gene transfer and the evolution of methanogenic pathways. *Horizontal gene transfer: genomes in flux (*Gogarten, M.B. ; Gogarten, J.P. ; Olendzenski, L., eds.), pp. 163-179. Humana Press.

480 Franzmann PD, Liu Y, Balkwill DL, Aldrich HC, Conway de Macairo W & Boone DR (1997)
481 *Methanogenium frigidum* sp. nov., a psychrophilic, H_2-using methanogen from Ace Lake,
482 Antarctica. *Int J Syst Bacteriol* **47**: 1068-1072.
483 Friedmann EI (1994) Permafrost as microbial habitat. *Viable microorganisms in Permafrost.*
484 (Gilichinsky DA, ed.) pp. 21-26. Russian Academy of Science, Pushchino.
485 Fung I, John J, Lerner J, Matthews E, Prather M, Steele LP & Fraser PJ (1991) Three-dimensional
486 model synthesis of the global methane cycle. *J Geophysical Res* **96**: 13033-13065.
487 Giaquinto L, Curmi PMG & Siddiqui KS (2007) Structure and function of cold shock proteins in
488 Archaea. *J Bacteriol* **189**: 5738–5748.
489 Gilichinsky DA, Soina VS & Petrova MA (1993) Cryoprotective properties of water in the Earth
490 cryolithosphere and its role in exobiology. *Origins Life Evol Biosphere* **23**: 65 - 75.
491 Harz M, Rösch P & Popp J (2009) Vibrational spectroscopy- a powerful tool for the rapid
492 identification of microbial cells at the single-cell level. *Cytometry Part A* **75A**: 104-113.
493 Hedderich R & Whitman W (2006) *Physiology and biochemistry of methane-producing archaea*.
494 Springer Verlag, New York.
495 Helm D, Labischinski H & Naumann D (1991) Elaboration of a procedure for identification of
496 bacteria using Fourier-transform infrared spectral libraries: A stepwise correlation approach.
497 *J Microbiol Methods* **14**: 127-147.
498 Hermelink A, Brauer A, Lasch P & Naumann D (2009) Phenotypic heterogeneity within
499 microbial populations at the single-cell level investigated by confocal Raman
500 microspectroscopy. *Analyst* **134**: 1149–1153.
501 Hoover RB & Pikuta EV (2009) Psychrophilic and psychrotolerant microbial extremophiles in
502 polar environments. *Polar microbiology* (Bej AK, Aislabie J & Atlas R, eds.), pp. 115 -156.CRC
503 Press.
504 Imhoff-Stuckle D & Pfennig N (1983) Isolation and characterization of a nicotinic acid-
505 degrading sulfate-reducing bacterium, *Desulfococcus niacini* sp. nov. *Arch Microbiol* **136**: 194–
506 198.
507 Ivleva NP, Wagner M, Horn H, Niessner R & Haisch C (2009) Towards a nondestructive
508 chemical characterization of biofilm matrix by Raman microscopy. *Anal Bioanal Chem* **393**:
509 197-206.
510 Jain R, Rivera MC & Lake JA (1999) Horizontal gene transfer among genomes: The complexity
511 hypothesis. *PNAS* **96**: 3801–3806.
512 Krause M, Rösch P, Radt B & Popp J (2008) Localizing and identifying living bacteria in an
513 abiotic environment by a combination of Raman and fluorescence microscopy. *Anal Chem* **80**:
514 8568–8575.
515 Kurr M, Huber R, König H, Jannasch HW, Fricke H, Trineone A, Kristjansson JK & Stetter KO
516 (1991) *Methanopyrus kandleri*, gen. and sp. nov. represents a novel group of
517 hyperthermophilic methanogens, growing at 110°C. *Arch Microbiol* **156**: 239-247.
518 Liu Y & Whitman W (2008) Metabolic, phylogenetic, and ecological diversity of the
519 methanogenic archaea. *Ann NY Acad Sci* **1125**: 171-189.
520 Luton PE, Wayme JM, Sharp RJ & Riley PW (2002) The mcrA gene as an alternative to 16S rRNA
521 in the phylogenetic analysis of populations in landfill. *Microbiol* **148**: 3521-3530.
522 Maestrojuan GM, Bonne JE, Mah RA, Menaia JAGF, Sachis MS & Boone DR (1992) Taxonomy and
523 halotolerance of mesophilic Methanosarcina strains, assignment of strains to species, and
524 synonymy of *Methanosarcina mazei* and *Methanosarcina frisia*. *Int J Syst Bacteriol* **42**: 561-
525 567.
526 Mah RA (1980) Isolation and characterization of of *Methanococcus mazei*. *Current Microbiology*
527 **3**: 321- 326.
528 Maquelin K, Choo-Smith L-P, Kirschner C, Ngo Thi NA, Naumann D & Puppels GJ (2002)
529 Vibrational spectroscopic studies of microorganisms. *Handbook of vibrational spectroscopy,*
530 (Chalmers JM & Griffiths PR, eds.), pp. 3308 - 3334. John Wiley, Chichester.
531 Morozova D & Wagner D (2007) Stress response of methanogenic archaea from Siberian
532 permafrost compared with methanogens from non permafrost habitats. *FEMS Microbiol Ecol*
533 **61** 16–25.

534 Morozova D, Möhlmann D & Wagner D (2007) Survival of methanogenic archaea from Siberian
535 permafrost under simulated martian thermal conditions. *Orig Life Evol Biosph* **37**: 189–200.
536 Morozova D, Moeller R, Rettberg P & Wagner D (2015) Enhanced radiation resistance of
537 *Methanosarcina soligelidi* SMA-21, a new methanogenic archaeon isolated from a Siberian
538 permafrost-affected soil in direct comparison to *Methanosarcina barkeri*. *Astrobiology* **15**:
539 Naumann D (2000) Infrared spectroscopy in microbiology. *Encyclopedia of Analytical*
540 *Chemistry: applications, theory and instrumentation.* (Meyers R., ed), pp. 102-131. John Wiley
541 and Sons Ltd, Chichester.
542 Neugebauer U, Schmid U, Baumann K, Zieburh W, Kozitskaya S, Deckert V, Schmitt M & Popp J
543 (2007) Towards a detailed understanding of bacterial metabolism- spectroscopic
544 characterization of *Staphylococcus epidermidis*. *Chem Phys Chem* **8**: 124-137.
545 Ophir T & Gutnick D (1994) A role for exopolysaccharides in the protection of microorganisms
546 for dessication. *Appl Environ Microbiol* **60**: 740-745.
547 Pereira R, Martin AA, Tierra-Criollo CJ & Santos I (2004) Diagnosis of squamous cell carcinoma
548 of human skin by Raman spectroscopy. *Proceedings of SPIE* **5326**: 106 - 112.
549 Poli A, Di Donato P, Abbamondi GR & Nicolaus B (2011) Synthesis, production, and
550 biotechnological applications of exopolysaccharides and polyhydroxyalkanoates by archaea.
551 *Archaea* **2011**: 1-13.
552 Reed CJ, Lewis H, Trejo E, Winston V & Evilia C (2013) Protein adaptations in archaeal
553 extremophiles. *Archaea* **2013**: 273-275.
554 Reeve JN (1992) Molecular biology of methanogens. *Annu Rev Microbiol* **46**: 165-191.
555 Rösch P, Harz M, Schmitt M*, et al.* (2005) Chemotaxonomic identification of single bacteria by
556 micro-Raman spectroscopy: application to clean-room-relevant biological contaminations.
557 *Appl Environ Microbiol* **71**: 1626–1637.
558 Schirmack J, Böhm M, Brauer C, Löhmannsröben HG, de Vera JP, Möhlmann D & Wagner D
559 (2013) Laser spectroscopic real time measurements of methanogenic activity under
560 simulated Martian subsurface analog conditions. *Planetary and Space Science* **98**:198-204
561 Serrano P, Wagner D, Böttger U, de Vera JP, Lasch P & Hermelink A (2014) Single-cell analysis
562 of the methanogenic archaeon *Methanosarcina soligelidi* from Siberian permafrost by means
563 of confocal Raman microspectroscopy for astrobiological research. *Planet Space Sci* **98**: 191-
564 197.
565 Simankova MV, Kotsyurbenko OR, Lueders T, Nozhevnikova AN, Wagner B, Conrad R &
566 Friedrich MW (2003) Isolation and characterization of new strains of methanogens from cold
567 terrestrial habitats. *Syst Appl Microbiol* **26**: 312-128.
568 Socrates G (2004) Alkane group residues: CH group. *Infrared and Raman characteristic group*
569 *frequencies Tables and charts.* (Socrates G., ed.), pp. 50-67. John Wiley and sons Ltd.,
570 Chichester.
571 Thauer RK, Kaster AK & Seedorf H (2008) Methanogenic archaea: ecologically relevant
572 differences in energy conservation. *Nat Rev Microbiol* **6**: 579-591.
573 The MathWorks, Inc. MATLAB and Statistics Toolbox Release 2014a. Natick, Massachusetts.
574 Thompson JD, Higgins DG & Gibson TJ (1994) CLUSTAL W: improving the sensitivity of
575 progressive multiple sequence alignment through sequence weighting, position specific gap
576 penalties and weight matrix choice. *Nucleic Acids Res* **22**: 4673 - 4380.
577 Vernikos GS & Parkhill J (2006) Interpolated variable order motifs for identification of
578 horizontally acquired DNA: revisiting the Salmonella pathogenicity islands. *Bioinformatics* **22**:
579 2196-2203.
580 Wagner D, Kobabe S, Pfeiffer E-M & Hubberten H-W (2003) Microbial controls on permafrost
581 fluxes from a polygonal tundra of the Lena Delta, Siberia. *Permafrost Periglac Process* **14**: 173-
582 185.
583 Wagner D, Lipski A, Embacher A & Gattinger A (2005) Methane fluxes in permafrost habitats of
584 the Lena Delta: effects of microbial community structure and organic matter quality.
585 *Environmental Microbiology* **7**: 1582-1592.

586 Wagner D, Schirmack J, Ganzert L, Morozova D & Mangelsdorf K (2013) *Methanosarcina*
587 *soligelidi* sp. nov., a desiccation and freeze-thaw resistant methanogenic archaeon isolated
588 from a Siberian permafrost-affected soil. *Int J Syst Evol Microbiol* **63**: 2986-2991.

589

Table 1. Description of the Raman bands identified in the spectra of the methanogenic strains from Siberian permafrost (*Ms. soligelidi* SMA-21, SMA-17 and SMA-27) and the mesophilic methanogens (*Ms. mazei* and *Ms. barkeri)* measured with an excitation wavelenght of 532nm. The values of the bands exclusive to one or a few strains are presented in grey. + indicates the presence of a certain band, and - its absence. Qualitative differences are indicated with the symbol (+), meaning a higher intensity of the peak and therefore cellular abundance.

Wavenumber (cm^{-1})	Description	Ms. mazei	Ms. barkeri	SMA-17	Ms. soligelidi SMA-21	SMA-27
2936	CH_3 str and CH_2 str	+	+	+	+	+
2885	CH_3 str sym	-	-	+	+(+)	+(+)
1669	amide I (C=O str, NH_2 bend, C=N str)	+(+)	+(+)	+	+	+(+)
1610	C=C (Phe, Tyr)	+ (+)	+ (+)	+	+	+
1589	G + A ring str (nucleic acids); Trp	+	+	-	-	-
1460	δ(CH2) scis, CH2 def	+	+	+	+	+
1344	δ(CH)	+(+)	+(+)	+	+	+(+)
1338	δ(CH)	-	-	+	+	-
1275-1243	Amide III	+(+)	+(+)	+	+	+(+)
1167	C–C, C–O ring breath, asym	+	+	+	+	+
1128	C–C str, C–O–C glycosidic link; ring breath, sym (carbohydrates); C–N, C–C str (proteins); C–C str (lipids)	+	+	+	+	+

1054	C–O, C–C str (carbohydrates); C–C; C–N (proteins)	+	+	+(+)	+(+)	+(+)
1008	n(CC) aromatic ring (Phe)	+	+	+(+)	+(+)	+(+)
860	C-C str; C-O-C glycosidic link	+	+	+(+)	+ (+)	+(+)
835	Ring breath Tyr; O–P–O str (DNA/RNA)	-	-	+	+	+

Figure Legends

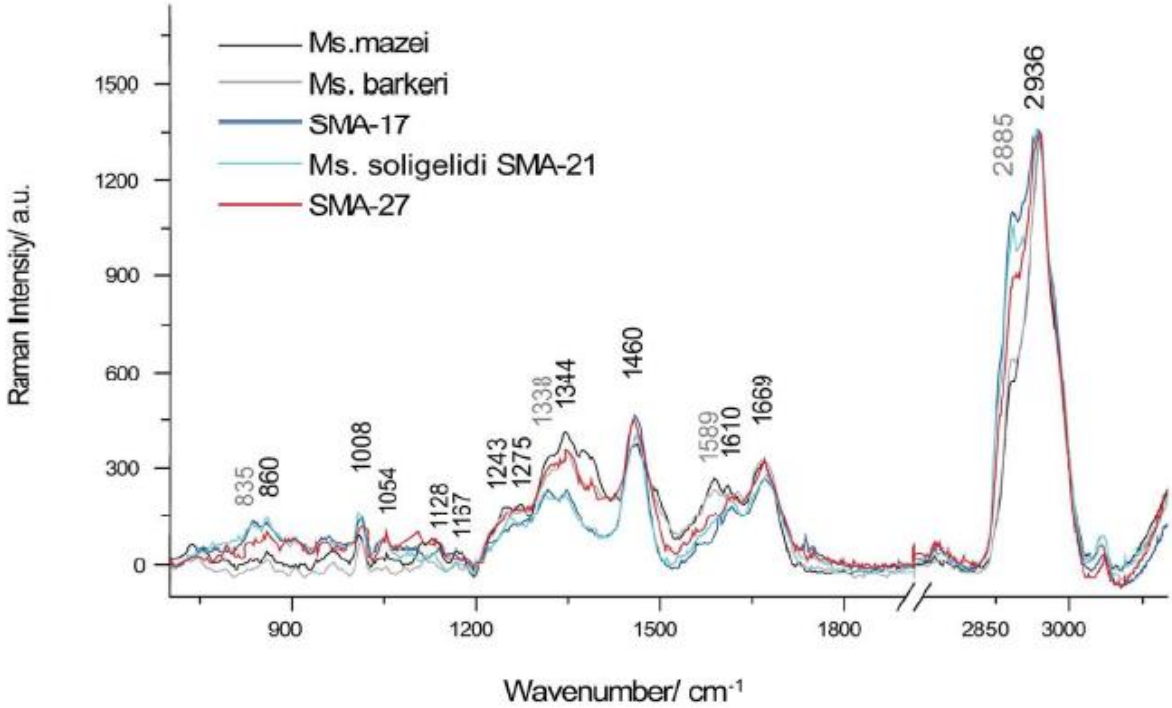

Figure 1. Average Raman spectra of methanogenic strains from Siberian permafrost (*Ms. soligelidi* SMA-21, SMA-17 and SMA-27) and non-permafrost environments (*Ms. mazei* and *Ms. barkeri)* measured with an excitation wavelength of 532nm. Note that values corresponding to the band positions specific to one or a few strains are presented in grey.

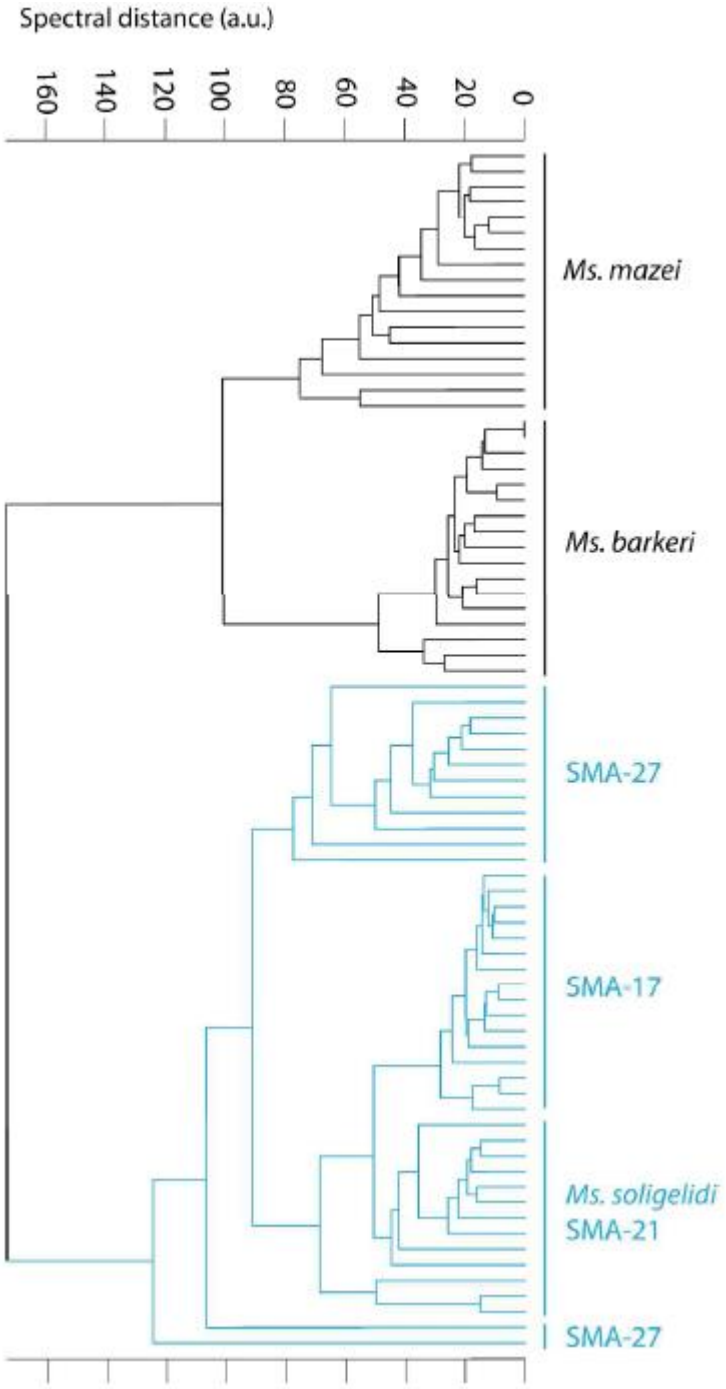

Figure 2. Cluster analysis (average linkage method) of Raman spectra from individual cells from permafrost and non-permafrost strains in stationary phase. CRM spectra from *Methanosarcina mazei* and *Ms. barkeri* (non-permafrost strains) form a cluster, which is well separated from the cluster of permafrost strains (SMA-27, *Ms. soligelidi* SMA-21 and SMA-17).

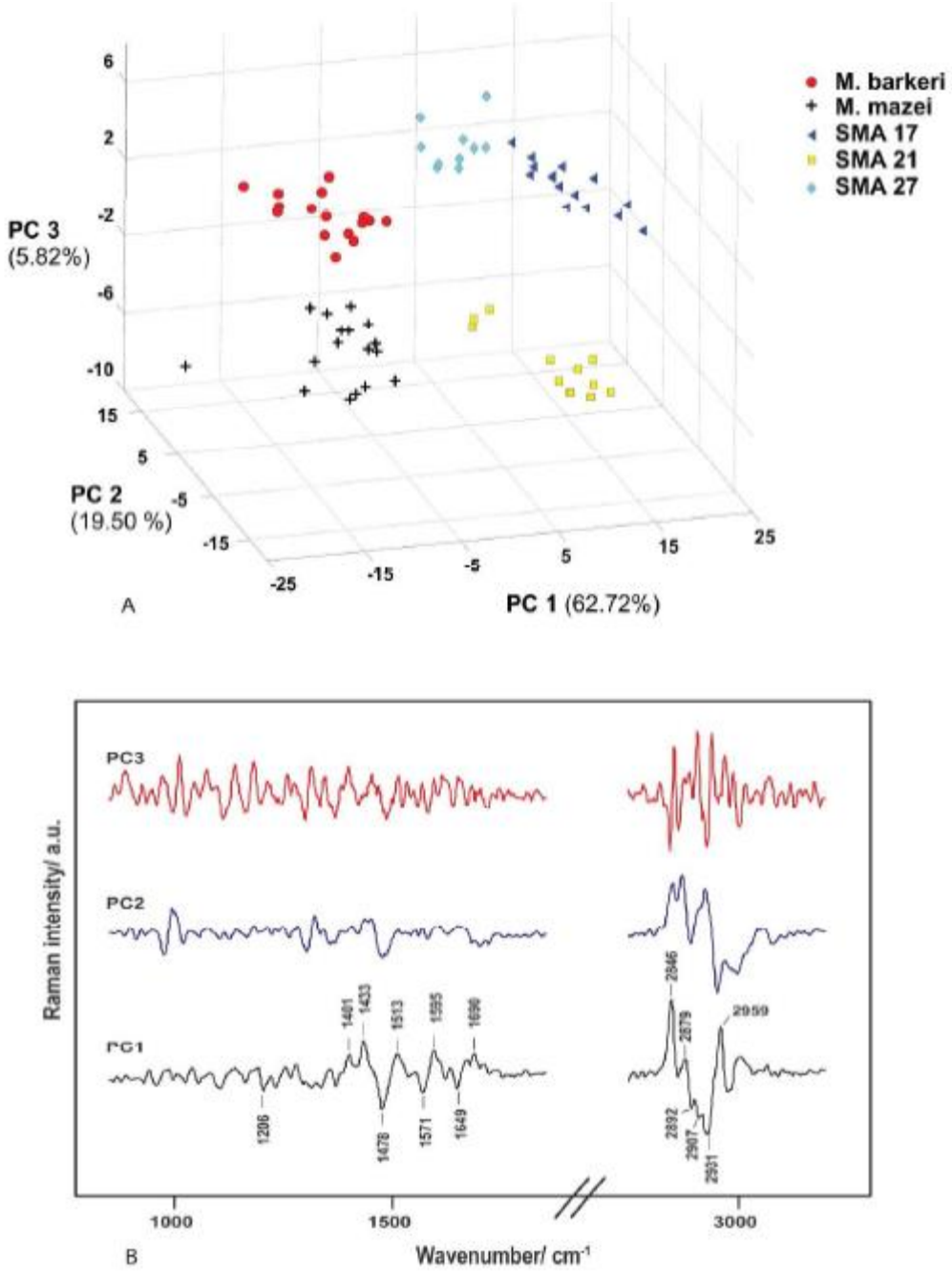

Figure 3. Principal Component Analysis (PCA) of the individual spectra of the five methanogenic strains (A) Score plot of the first 3 principal components (PCs) of the total variance of the spectra. (B) Loadings of the first three principal components, illustrating the major spectral differences in PC1 (labeled peaks).

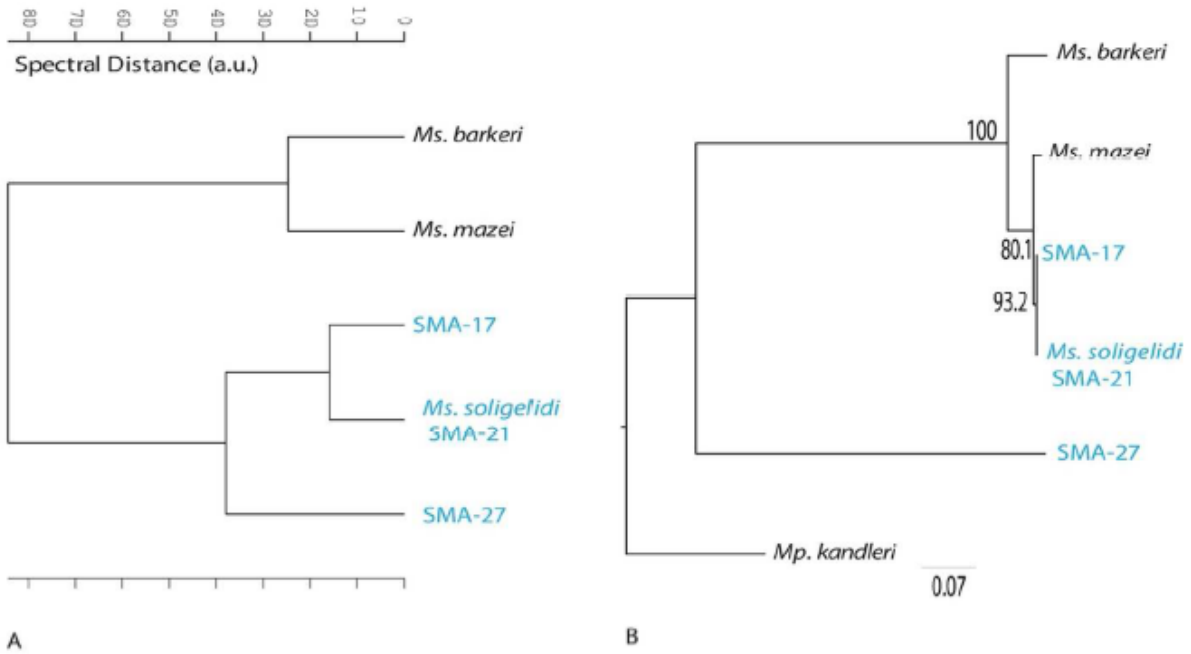

Figure 4. Chemical *vs*. phylogenetic relationships of methanogenic archaea from Siberian permafrost *Methanosarcina soligelidi* SMA-21, SMA-17 and SMA-27 (in blue) and the two non-permafrost strains used as reference *Ms. barkeri* and *Ms. mazei* (A) Cluster analysis of the average Raman spectra from permafrost and non-permafrost strains in stationary phase using the average linkage clustering method. (B) Maximum likelihood tree (GTR substitution model, 1000 bootstraps) according to the mcrA nucleotide sequence. *Methanopyrus kandleri* (*Methanopyrales*) was used as the outgroup. The branch support values indicated in the nodes show the robustness of the phylogenetic reconstruction.